Proceedings of the 3rd Croatian Conference on Earthquake Engineering - 3CroCEE
19–22 March 2025, Split, Croatia

DOI: https://doi.org/10.5592/CO/3CroCEE.2025.111

NUMERICAL EXPERIMENT FOR SHEAR KEY JOINT BEHAVIOUR SIMULATION IN ARCH DAMS: PART 1 – INVESTIGATING THE INFLUENCE OF THE KEY SHAPE AND ANGLE

Ana Nanevska [(1)], Violeta Mircevska [(2)]

[(1)] *Research Assistant, Institute of Earthquake Engineering and Engineering Seismology, University of Ss. Cyril and Methodious, Skopje, R. N. Macedonia., nanevska@iziis.ukim.edu.mk*
[(2)] *Professor, Institute of Earthquake Engineering and Engineering Seismology, University of Ss. Cyril and Methodious, Skopje, R. N. Macedonia., mircevska@iziis.ukim.edu.mk*

Abstract

Nonlinear behaviour of contraction joints in arch dams, such as joint opening and sliding caused by hydrostatic pressure and temperature variations can affect the dam's serviceability. Furthermore, strong seismic events can additionally alter the response in dynamic conditions, impacting the natural period and stress redistribution in the arches and cantilevers. In order to enhance structural integrity with additional shear strength, shear key elements are usually installed along these joints. However, traditional modeling with the actual shear key geometry results in complex analyses. This paper presents a novel approach for simulating shear key behaviour by modifying the flat joint concept in ADAD-IZIIS software. The method introduces additional tangential stiffness to the flat joint's stiffness matrix to simulate shear resistance derived from the key geometry. The model uses a uniaxial constitutive law for nonlinear behaviour in normal and Coulomb's friction law in the tangential direction. This paper presents the first part of a comprehensive study examining the influence of the key shape and angle through numerical experiments using refined FE models of flat, bevelled, and unbevelled shear key joints. The additional shear resistance $F_{\tau,add}$ is calculated by increasing the initial modulus of elasticity $E_{n,\tau}$ in the local shear direction as $E_{n\tau,add}=k_{ad}*E_{n,\tau}$, applying the additional tangential stiffness coefficient k_{ad}, derived from the experimental analyses. Results indicate that the shape and angle of the key greatly influence the element's shear resistance. Unbevelled shear key joint increases tangential stiffness by approximately 60%, while the bevelled joint by 23% compared to the flat joint. Although tangential stiffness minimally affects the extreme joint openings at the top edge, the unbevelled joint significantly reduces openings along the joint length. The research confirms the efficiency of the proposed approach in simulation of the complex nonlinear behavior of an arch dam constructed with shear key joints.

Keywords: contraction joint, nonlinear behaviour, shear key, numerical experiment.

1. Introduction

Arch dams are highly efficient structures that transfer large compressive stresses to the supports through their curved arch geometry [1]. In order to control tensile stresses development caused by expansion and contraction during concreting, temperature variations, as well as seismic activity, arch dams are constructed in monolithic blocks separated by vertical joints [2]. These joints, however, are potential weak points due to imperfections in the grouting process, making them susceptible to initial damage from temperature variations and strong earthquakes [3]. During strong earthquakes, the monoliths undergo relative displacements, resulting in joint opening and shear sliding, causing significant redistribution of internal forces both during the seismic action and afterward due to residual joint openness. Several studies [4][5][6][7][8] have demonstrated that the nonlinear behaviour of these joints in arch dams, including their opening and shear sliding increases the natural period of the dam and leads to a significant redistribution of stresses in the arches and cantilevers. Therefore, accurate numerical simulation of these behaviours is critical for evaluating the static and seismic stability of arch dams.

To improve the compactness, shear strength and enhance the overall integrity of arch dams, shear key elements are often incorporated along the joints in the radial and/or longitudinal directions. These elements are designed to provide additional shear resistance when joints experience normal

Proceedings of the 3rd Croatian Conference on Earthquake Engineering - 3CroCEE
19–22 March 2025, Split, Croatia

DOI: https://doi.org/10.5592/CO/3CroCEE.2025.111

displacements, i.e. opening in the normal direction [9]. While shear keys offer significant advantages, including improved monolithic integrity particularly in thinner arch dams, their analytical modeling remains challenging. Despite advancements over the last four decades, comprehensive analysis of arch dams with shear key joints remains limited. Namely, over the past four decades, number of different constitutive models have been applied for joint behaviour simulation, progressing from models that include only the normal displacement of joints, to models that include the relationship between the opening and shear sliding in the contact.

Early modeling efforts include contact elements derived from rock mechanics, such as finite elements for soft material contacts that do not work in tension [10][11][12]. Beer, 1985 [13] developed a contact element using special quasi-continuum finite elements with a small thickness and a prescribed reduced stiffness. However, further studies are needed to extend the applicability of this method for simulation of dynamic behaviour. Further developments introduced nonlinear spring models [14], which also failed to incorporate the most important mechanical properties of the shear key elements, including initial tensile stresses from grouting and shear strength loss due to dilation. Later studies incorporating 3D contact elements were limited to simulating the behaviour of the joint in the normal direction only, neglecting the interaction effects between normal and tangential displacements [4]. The first FE models with a discrete crack in the joint were developed for tensile failure for a prescribed lower limit only for static load [15] or not considering all physical properties of the joint [16].

A gap element introduced into the ADINA software assumed identical movement of contact element points in the vertical and radial directions, an assumption that does not align with the observed behaviour of shear key joints [17]. Similarly, a nonlinear contact element incorporated in the ADAP-88 software considered both normal and tangential displacements but didn't consider the geometric characteristics of the shear key elements [18]. Another approach employed a zero-thickness contact element to model structural joints, considering opening, closing, and shear effects, as well as limiting relative tangential displacements based on a predefined slip limit specified according to the joint's geometry [5]. While this method achieves satisfactory accuracy for prevented slip in the contact, under conditions of partial slip with partial joint openness its efficiency needs to be improved.

The discrete crack contact model proposed by Ahmadi et al., 2001 [3] was used to capture the nonlinear interaction between shear and tension behavior, making it an important advancement in understanding the key mechanical properties of joints. This model incorporates partial tangential sliding that depends on normal displacements, assuming elastic behavior for closed joints and fully plastic behavior when the shear strength is exceeded. Additional efforts to model contact elements include elements with zero thickness [19] as well as linear springs [20], both of which ignore the most important shear key effects. More precise joint configurations have been adopted in numerical simulations to achieve realistic representations of shear key joint behaviour [21]. However, analyses' results show significant stress concentrations at sharp contact angles, that highlights the need for further model refinements. Additional developments, such as the introduction of additional tangential nonlinear spring elements with enhanced stiffness to simulate shear key effects address some of these challenges [22]. Still, further improvements remain necessary, as current models lack comprehensive consideration of different shear key geometries.

Simulating the nonlinear behavior of joints presents a significant challenge, particularly in accounting for all influencing factors and addressing computational limitations. A major difficulty is accurately modeling of the complex shear key geometry, as the dense finite element mesh required for precise representation often leads to computational impracticalities. To address this, it is necessary to develop a constitutive law that will integrate the effect of material nonlinearity of the grouting mass with the restrictive shear effect of the shear key geometry. In this study, a nonlinear constitutive model for simulating the behavior of shear key joints is developed. The model integrates existing research insights and introduces modifications based on numerical experiments to accurately replicate shear key behavior. The model is based on a 3D flat joint contact element previously integrated into the ADAD-IZIIS software [23]. This paper presents the first part of a comprehensive study, focusing on results of

DOI: https://doi.org/10.5592/CO/3CroCEE.2025.111

numerical experiments that investigate the influence of the key shape and angle on the behaviour of shear key joints in arch dams.

2. 3D flat contact element implemented in the ADAD-IZIIS software

The flat joint behaviour in the software [23] is simulated using a 3D contact element positioned between two adjacent finite elements (representing concrete monoliths) with different mechanical properties. The finite elements can be modelled with 6, 8, 15 or 20 points, while the contact elements with 6, 8, 12 or 16 points. Each pair of nodes has identical global coordinates, with one node on the lower contact surface (Π1) and the corresponding node on the upper contact surface (Π2). Fig. 1 illustrates these contact surfaces, representing the faces of two different finite elements in the contact, each defined by eight points.

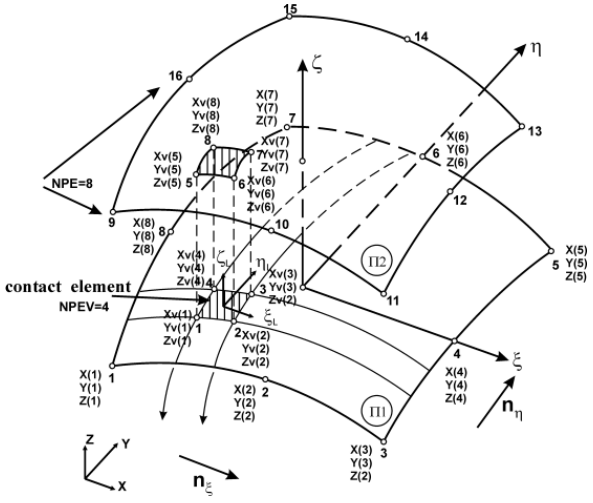

Figure 1. Schematic representation of the 8-point contact element

The contact element follows a uniaxial constitutive law for the nonlinear behaviour in the normal direction (Fig. 2a) and Coulomb's law of friction for the two tangential directions (Fig. 2b), capturing a coupled effect of the stresses in all three directions of the contact. The mechanical properties of the grouting mass are adopted with slightly lower values than the concrete in the monoliths, namely: modulus of elasticity in the normal and tangential directions $E=25.5*10^7$ kPa, tensile strength $\sigma_{t,doz}=1000$ kPa, compressive strength $\sigma_{c,doz}=25500$ kPa, compressive dilation $\varepsilon_c=0.2*10^{-3}$ m, compressive dilation $\varepsilon_{fail}=0.3*10^{-3}$ m when the compressive strength drops to $\sigma_{c,fail}=20\ 000$ kPa and shear strength $\tau=2000$ kPa. The monoliths assume linear behaviour of concrete corresponding to C25/30, with the following characteristics: modulus of elasticity $E_n=31.5*10^7$ kPa, Poisson's ratio $\nu=0.2$ and bulk density $\gamma_{con}=24.0$ kN/m^3.

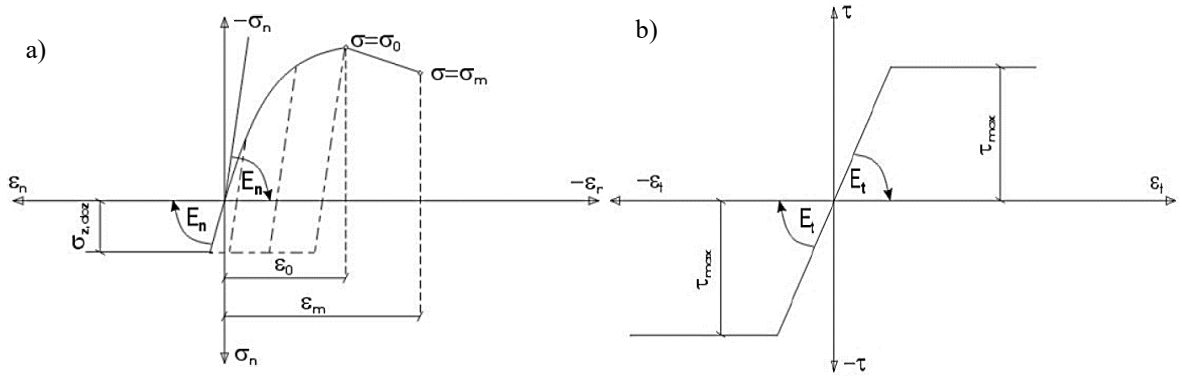

Figure 2. Constitutive relations for the behaviour of the grouting mass in construction joints in the a) normal direction and b) two tangential directions

DOI: https://doi.org/10.5592/CO/3CroCEE.2025.111

3. Numerical experiment for shear key joint behaviour simulation in arch dams

The simulation of shear key joint behaviour in the study incorporates modifications to the flat element concept in the tangential direction, introducing additional shear resistance that is induced by the geometric shear resistance of the shear key element. Further key assumptions are:

1. The tangential shear resistance combines the Coulomb's friction force, and an additional shear resistance attributed to the shear key geometry when the element is activated:

$$F\tau = F\tau_f + Fc + F\tau_{ad} = (\mu\sigma_n + c) + F\tau_{ad} \quad (1)$$

2. When the joint opens, the shear resistance depends solely on the joint's geometry until shear failure occurs within the key.
3. The behaviour of shear key joints results from the interaction between relative normal and tangential stresses.
4. The additional tangential force is obtained by increasing the initial modulus of elasticity in the direction of the shear key element. The increased modulus of elasticity $E_{1\,\tau,add}$ is expressed as:

$$E_{1\,\tau,add} = k_{ad} * E_{1,\tau} \quad (2)$$

where k_{ad} is the additional tangential stiffness coefficient, and $E_{1,\tau}$ is the initial tangential modulus of elasticity. The coefficient k_{ad} is determined through numerical experiments using three very refined finite element models, one with a flat joint configuration (Model 1, Fig. 3 a), and two models with different geometry of the shear key joint, a bevelled shear key joint with a 30° angle (Model 2, Fig.3 b) and an unbevelled shear key joint (Model 3, Fig. 3 c). These models enable the quantification of the additional stiffness effects influenced by the shear key geometry, its shape and key angle.

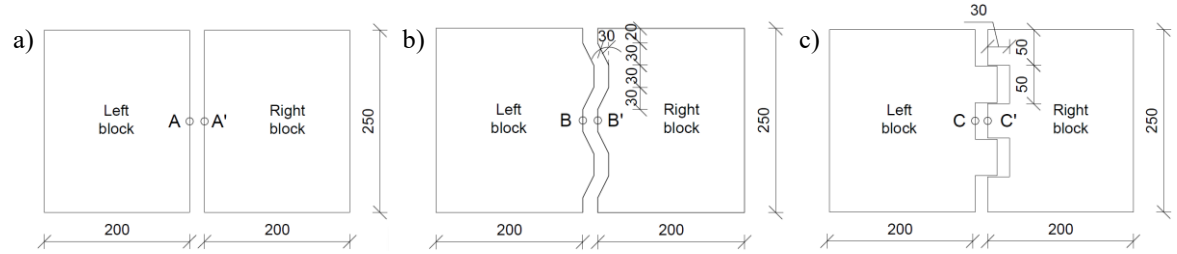

Figure 3. Geometric characteristics: a) Model 1, b) Model 2, and c) Model 3

Fig. 4 shows the finite element mesh and boundary conditions applied to the analysed models. In each configuration, the left side is fixed, while a horizontal static force is applied incrementally in 20 steps on the right side. The force is incremented according to the linear relation $F_{fmi} = F_s * f_{mi}$, where the multiplier f_{mi} ranges from 1 to 50, while the horizontal static force applied at the first loading step has a magnitude of 25000 kN. The experiment is conducted until the uniaxial compressive strength in the contact's normal direction is reached. For Models 2 and 3, a constant tangential modulus of elasticity is adopted, while for Model 1 different coefficients of additional tangential stiffness k_{ad} are applied until the contact slip values between the flat joint and shear key joints coincide. This approach easily determines the values of k_{ad} that effectively replicate the shear resistance effects induced by the shear key geometry, allowing these effects to be easily incorporated into the flat joint model.

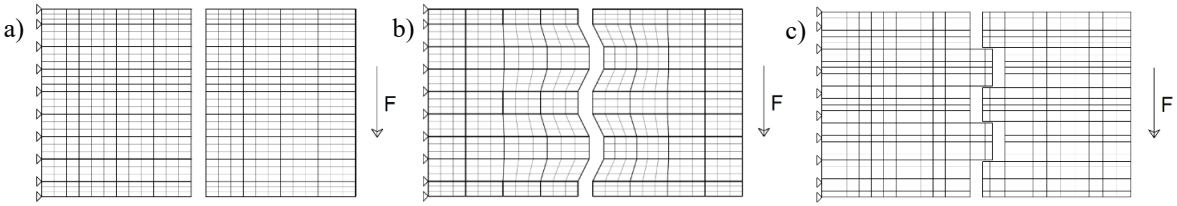

Figure 4. Finite element mesh and boundary conditions for: a) Model 1, b) Model 2 and c) Model 3

DOI: https://doi.org/10.5592/CO/3CroCEE.2025.111

4. Results from numerical experiments

The conducted numerical experiments in the first part of this study offer a comprehensive evaluation of the behaviour of different types of shear key joints compared to flat joints under incremental loading conditions. The shear key joints are analysed separately and compared with the flat joint, using various coefficients of additional tangential stiffness k_{ad}. For the bevelled shear key (Model 2) comparisons were made with the flat joint (Model 1) using coefficients k_{ad}=1.0 (equal tangential stiffness for both models), k_{ad}=1.08, k_{ad}=1.18 and k_{ad}=1.23. For the unbevelled shear key joint (Model 3), coefficients with values of k_{ad}=1.0, k_{ad}=1.23, k_{ad}=1.49 and k_{ad}=1.60 were adopted for the flat joint (Model 1).

Fig. 5 shows the horizontal displacements in the monolithic blocks in both global directions for incremental load factor f_{mi}=50: a) Model 1 with k_{ad}=1.0, b) Model 2 and c) Model 3. Fig. 6 illustrates the zones of open contact elements in the joints for the same load factor (f_{mi}=50) for Model 1 with k_{ad}=1.0, Model 2 and Model 3. For all joint types, the concentration of open elements occurs predominantly in the upper half of the contact zone, which aligns with the action of a bending force. The stress-strain relationships for all models are shown in Fig. 7, focusing on the contact elements where extreme responses occur. The figure shows the stress-strain relationships for: Model 1 with k_{ad}=1.0 in the contact elements in which the maximum: a) opening in the direction of the normal (CE 586) and b) sliding in the direction of the shear key element (CE 275) occur; Model 2 in the contact elements in which the same extremes occur, shown in the corresponding elements: c) CE 586 and d) CE 132 and Model 3 in the contact elements where the extremes occur: e) CE 370 and f) CE 617. Each figure also highlights the position of these elements.

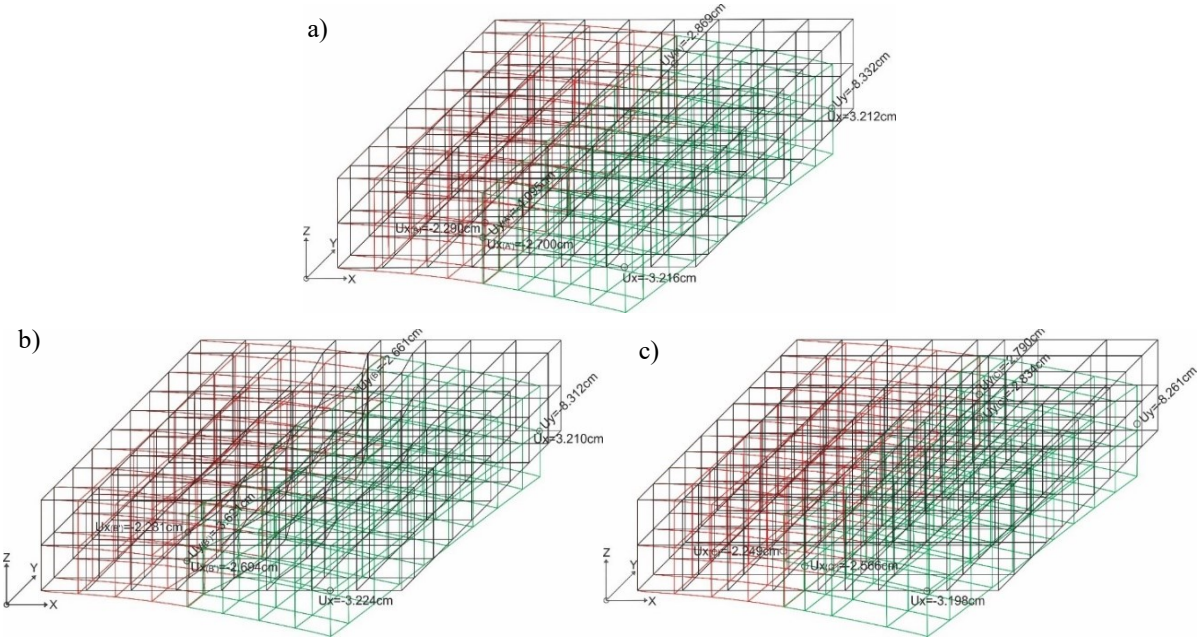

Figure 5. Horizontal displacements in the monoliths in both global directions (f_{mi}=50): a) Model 1 with k_{ad}=1.0, b) Model 2 and c) Model 3

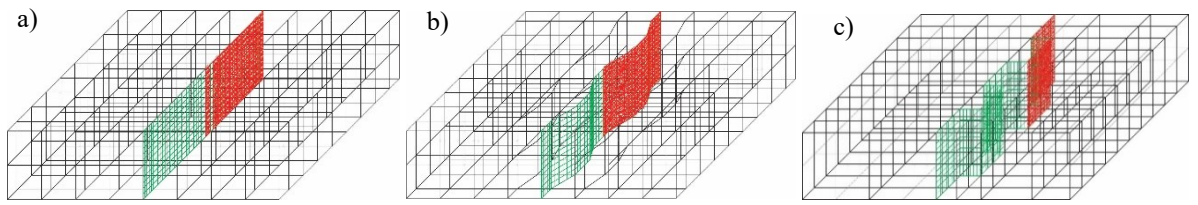

Figure 6. Open contact elements (f_{mi}=50): a) Model 1 with k_{ad}=1.0 (46% open elements), b) Model 2 (45% open elements) and c) Model 3 (35% open elements)

DOI: https://doi.org/10.5592/CO/3CroCEE.2025.111

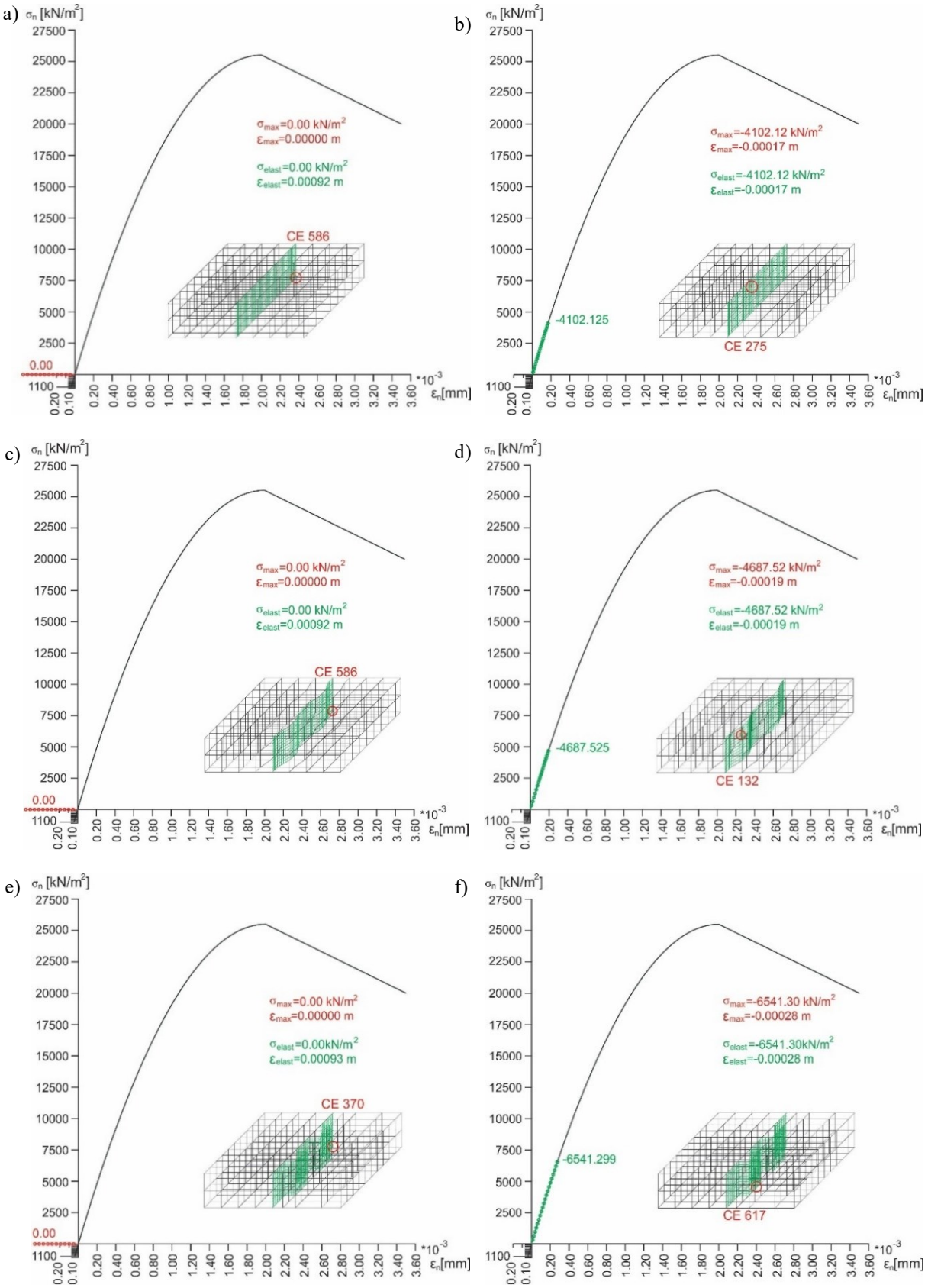

Figure 7. Normal stress–strain relationship (f_{mi}=50) in Model 1 (k_{ad} =1.0) for elements with maximum: a) opening in the direction of the normal (CE 586), b) sliding in the direction of the element (CE 275); Model 2: c) opening (CE 586), d) sliding (CE 132); and Model 3: e) opening (CE 370) and f) sliding (CE 617)

Proceedings of the 3rd Croatian Conference on Earthquake Engineering - 3CroCEE
19–22 March 2025, Split, Croatia

DOI: https://doi.org/10.5592/CO/3CroCEE.2025.111

The histories of maximum values of characteristic parameters, including shear sliding deformations, contact openings and horizontal displacements in the left and right monolithic blocks in the global y-direction are shown in Fig. 8 to Fig. 11. These parameters are calculated as functions of the incremental loading factor for Models 2 and 3 (shear key joints) and Model 1 (flat joint) with all coefficients of additional tangential stiffness k_{ad}. The results highlight significant differences in behaviour between the models.

The largest differences between the two models that are compared are in the contact shear sliding deformations. According to Fig. 8, the largest differences occur between Model 1 with k_{ad}=1.0 and Models 2 and 3, i.e. when all models have equal modulus of elasticity in the tangential direction. The maximum sliding deformation in the bevelled shear key joint (Model 2) is γ_{max}=0.87 mm, 24% smaller than the maximum deformation observed in the flat joint (γ_{max}=1.14 mm), Fig. 8a. For the unbevelled shear key joint (Model 3), the maximum sliding deformation is γ_{max}=0.54 mm, more than 50% smaller than the slip in the flat joint, Fig 8b. As the coefficient k_{ad} increases, the maximum sliding values in the flat joint converge towards those in the shear key joints. A good agreement in the values between the flat and bevelled shear key joints is achieved for k_{ad}=1.23, and between the flat and unbevelled shear key joints for k_{ad}=1.60. These shear sliding extremes for all types of joints occur near the middle of the contact zone (Figure 7b, d, f), immediately after maximum opening zones (Figure 6), consistent with the applied boundary conditions and forces.

Insignificant differences in values of maximum opening are observed across all models, with δ_{max}=0.923 mm for Model 2, δ_{max}=0.926 mm for Model 3, and δ_{max}=0.924 mm for Model 1 with k_{ad}=1.0 (Figure 9). This indicates that under pure bending loads, the additional tangential stiffness has a minimal impact on the maximum joint opening. Shear key joints (Models 2 and 3) exhibit increased tangential stiffness, resulting in dominant opening behaviour over sliding. For Model 1, as the loading factor f_{mi} exceeds 30, sliding deformations become more pronounced due to plastic yielding after exceeding the allowable shear stress. The maximum openings occur at the upper edge of the contact zone (Figure 7a, c, d), where the bending curvature is uniform across all analysed models, explaining their similar behaviour. That's why it's also useful to discuss openings in other characteristic elements along the contact. Additional analyses of openings in three characteristic contact elements along the joint, at the first key, the mid-point of the contact, and the second key (not shown in the paper) reveal that the unbevelled shear key joint (Model 3) more significantly reduces contact openings compared to the bevelled joint (Model 2). The shear sliding deformation ratios between Model 2 and Model 1 are 9% for the first contact element, 0% for the second (mid-part element), and 3% for the third contact element. For Model 3, these slip ratios are 51%, 70% and 51% for the three points, respectively. The same can be concluded by analysing the open elements zones, 35% open elements in Model 3, compared to 45% in Model 2 and 46% in Model 1 with k_{ad}=1.0.

Horizontal displacements in both monolithic blocks show the largest differences when comparing models with equal tangential stiffness, with differences decreasing as k_{ad} increases. While values for the flat joint approach those of the shear key joints when k_{ad} increases, they do not fully converge. For all joint types, the left monolithic block shows smaller maximum displacements compared to the right block, as dictated by the boundary conditions. In Model 3, the maximum displacement in y-direction in the left block (u_y=27.90 mm) is slightly higher than in Model 2 (u_y=26.61 mm), though both are smaller than the displacements in the flat contact, Model 1 with k_{ad}=1.0 (u_y=28.69 mm), Fig. 10. In the right block, maximum displacements in y-direction are u_y=36.21 mm for Model 2 and u_y=28.34 mm for Model 3, both smaller than the flat joint (u_y=40.95 mm), Fig. 11. The relative horizontal displacements between the blocks are significantly smaller in Model 3 (Δu_y=0.45 mm) compared to Model 2 (Δu_y=9.61 mm), with both being smaller than Model 1 (Δu_y=12.26 mm). The bevelled shear key joint reduces relative displacement by 20%, while the unbevelled shear key joint achieves over a 90% reduction. These results align with the reduced shear sliding deformation and increased tangential stiffness of the unbevelled shear key joint.

DOI: https://doi.org/10.5592/CO/3CroCEE.2025.111

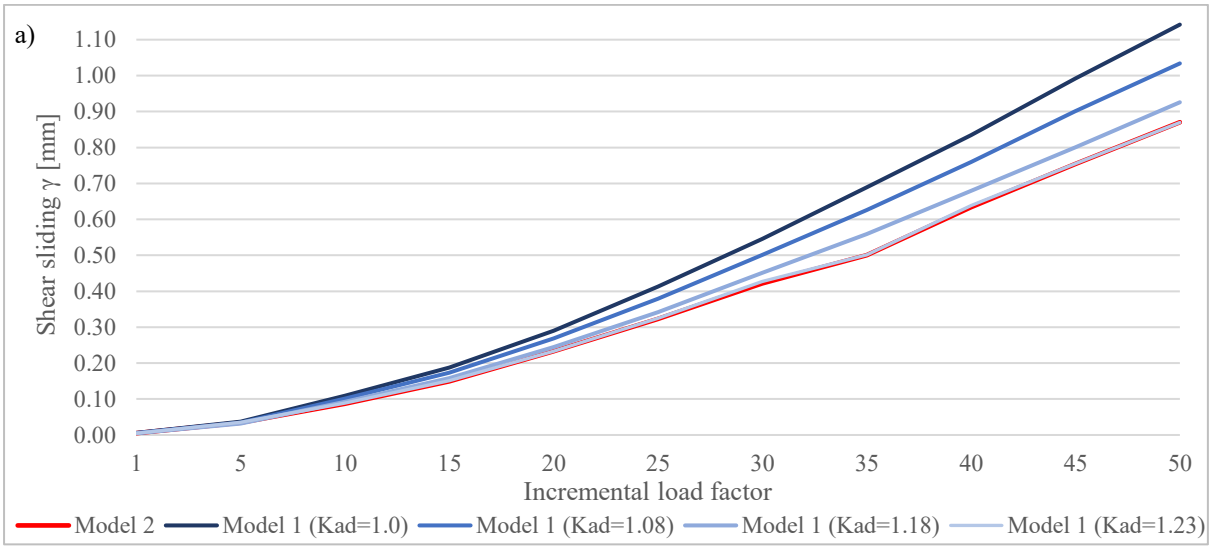

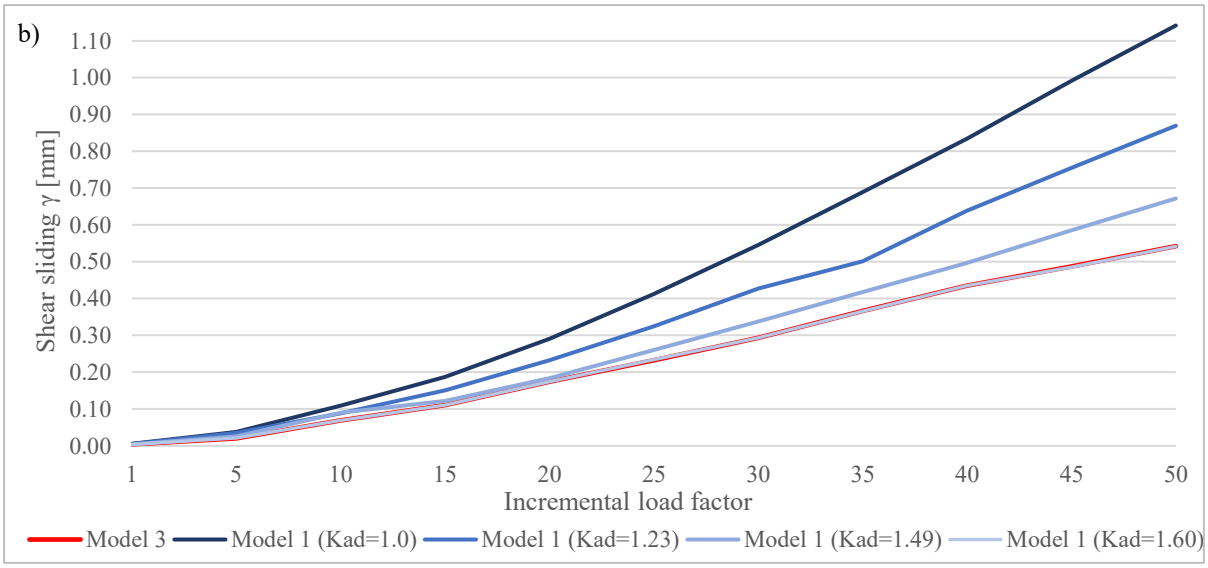

Figure 8. History of maximum shear sliding in the contact as a function of the incremental load factor for: (a) Model 1 and Model 2, (b) Model 1 and Model 3

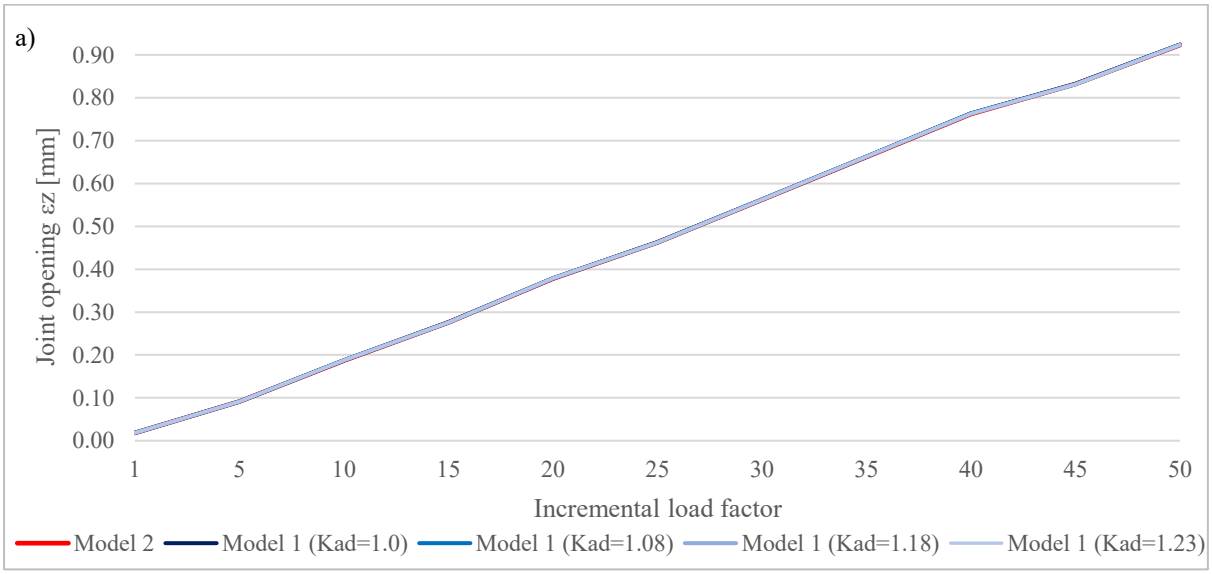

DOI: https://doi.org/10.5592/CO/3CroCEE.2025.111

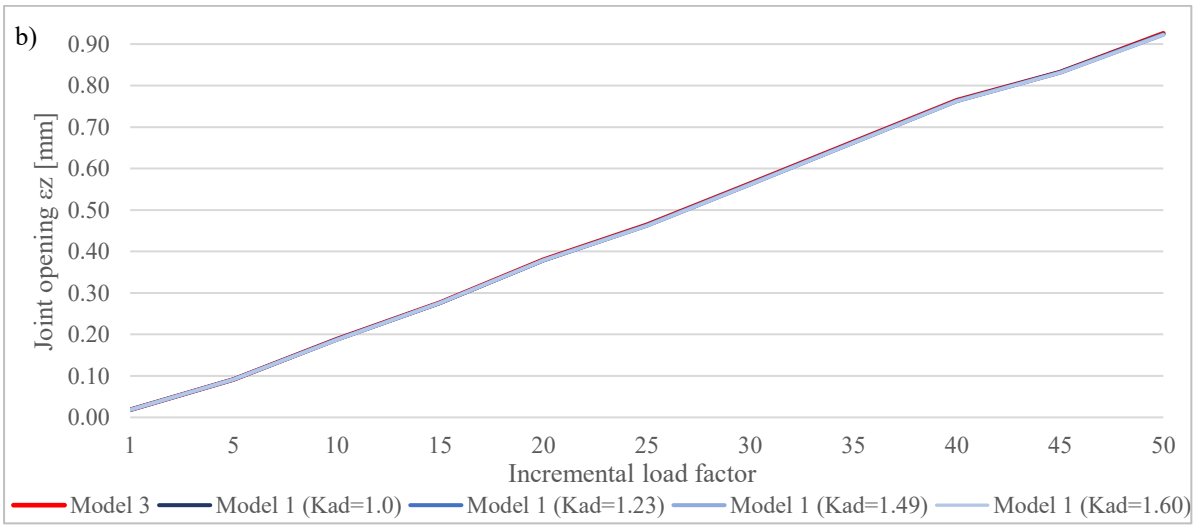

Figure 9. History of maximum opening in the contact as a function of the incremental load factor for: (a) Model 1 and Model 2 and (b) Model 1 and Model 3

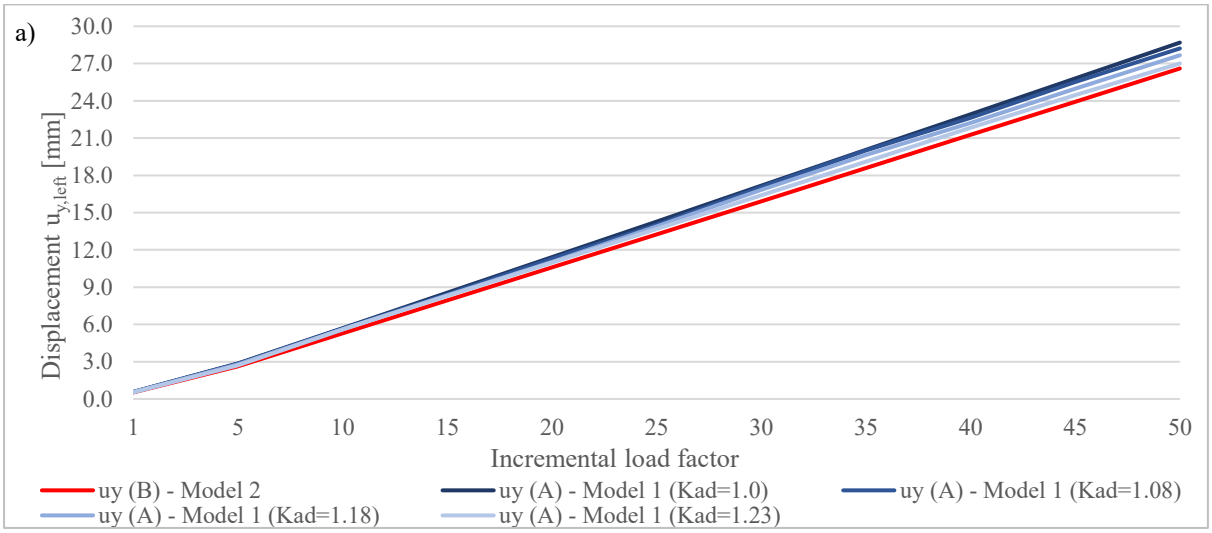

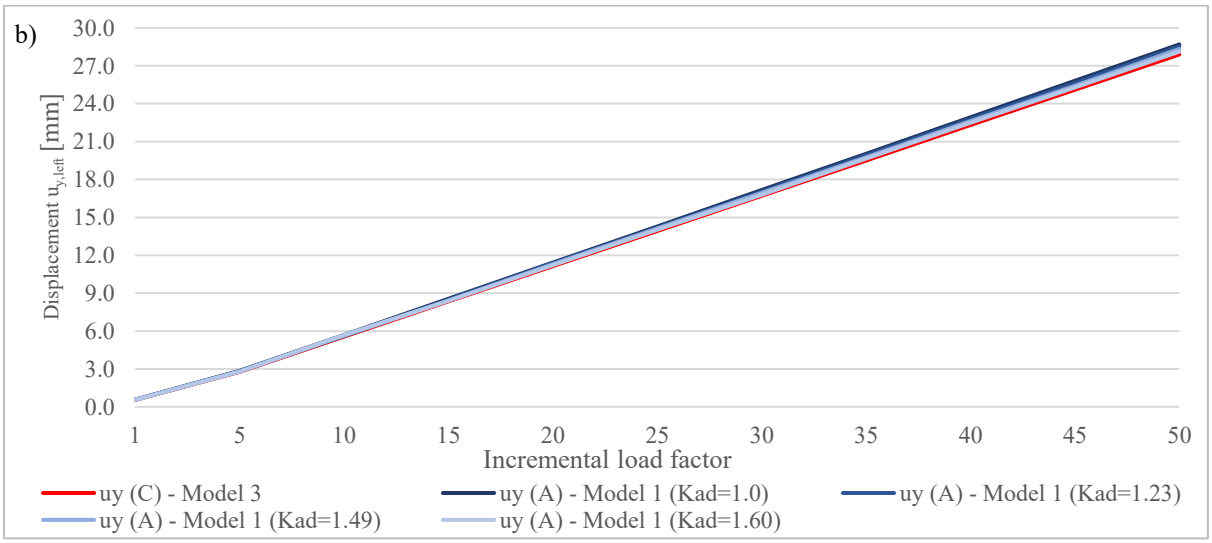

Figure 10. History of maximum horizontal displacements in the global y-direction in the left monolithic block as a function of the incremental load factor for: (a) Model 1 and Model 2 and (b) Model 1 and Model 3

DOI: https://doi.org/10.5592/CO/3CroCEE.2025.111

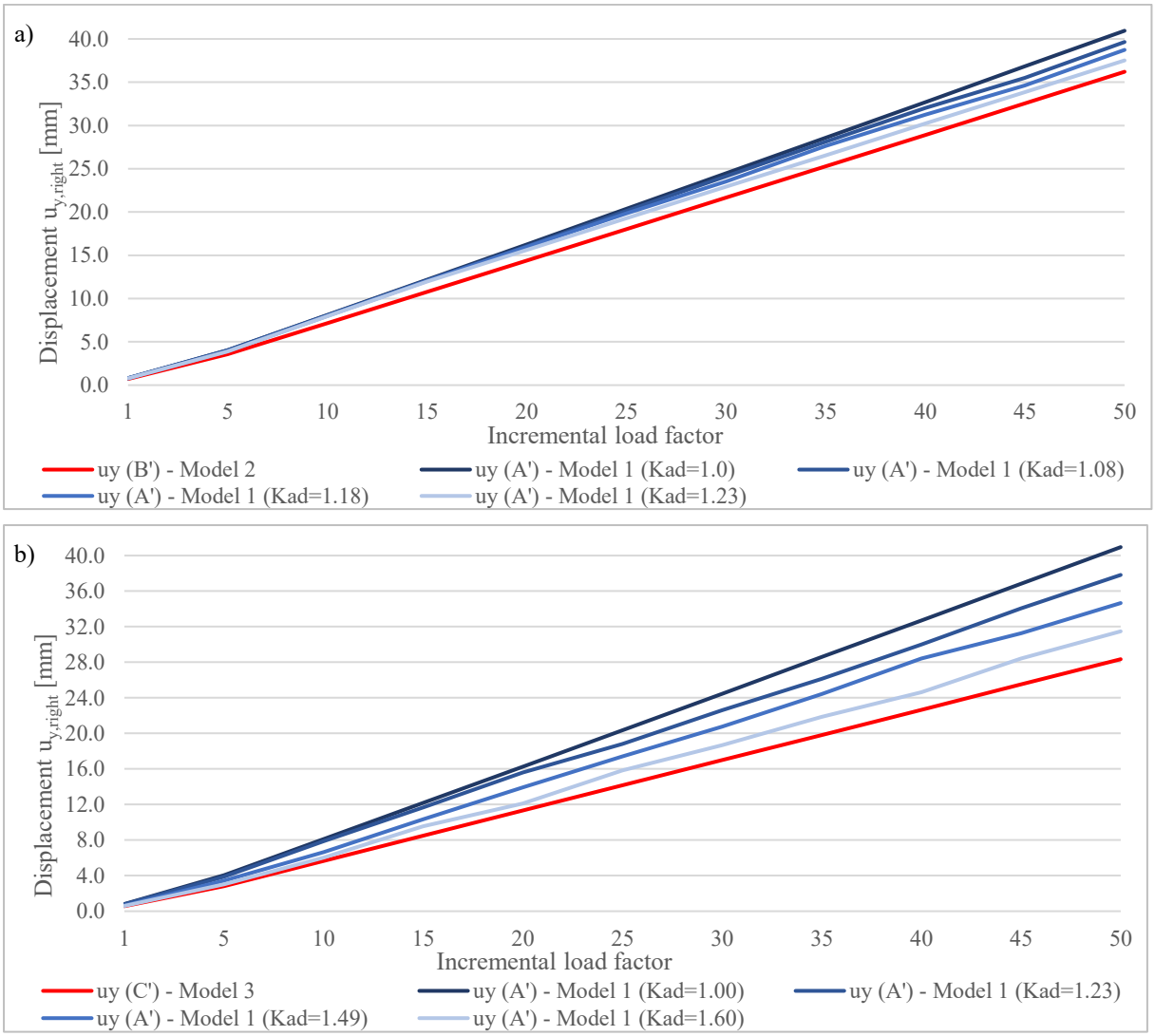

Figure 11. History of maximum horizontal displacements in the global y-direction in the right monolithic block as a function of the incremental load factor for: (a) Model 1 and Model 2 and (b) Model 1 and Model 3

5. Discussion of the results and conclusions

The aim of this research is to quantify the additional tangential stiffness representing the shear resistance of shear key joint elements with various geometries. The main focus is to derive these tangential stiffness values that can be applied to flat joints, thereby eliminating the need for detailed geometric modeling to capture the complexity of shear key joint geometry and behavior. These computed values, expressed as additional tangential stiffness coefficient are integrated into the flat joint contact elements' stiffness matrix, modifying the constitutive law to accurately simulate nonlinear behavior of the joint in the direction of the shear key elements, which may be implemented in one or two directions. The first part of the study focuses on the influence of shear key joint's geometry, with particular emphasis on key shape and angle.

The most pronounced differences among the analysed parameters are observed in the shear sliding deformations at the contact. The tangential stiffness coefficient k_{ad} is determined by equating the sliding deformations of the flat joint with various values of k_{ad}, to those observed in the shear key joints. The results indicate that replicating the shear resistance of the bevelled shear key joint requires a 23% increase in the tangential stiffness, while for the unbevelled shear key joint, an increase of 60% is

DOI: https://doi.org/10.5592/CO/3CroCEE.2025.111

needed. These findings underscore the significant impact of shear key geometry on the overall stiffness of the model, with each joint configuration contributing differently to the tangential resistance.

Despite different sliding behavior, all models exhibit nearly identical joint opening values, with the maximum occurring at the upper edge of the contact where the bending curve remains consistent across all models. This uniformity suggests that tangential stiffness has a negligible influence on the maximum joint opening. However, analyses of openings across different contact elements along the contact, reveal that the unbevelled shear key joint not only enhances tangential stiffness and shear sliding resistance, but also significantly reduces openings along the contact. Maximum horizontal displacements in the global y-direction within the contact zone, as well as relative displacements between the monolithic blocks, correspond closely to the observed shear sliding behavior. Furthermore, the response curves for all joint types demonstrate consistent trends across the analysed parameters.

The study findings confirm that the favourable shear key joint geometry (of both analysed types) significantly increases the tangential stiffness compared to flat joints. The geometry of the joints, particularly the shape and angle of the shear key element are key factors influencing the shear resistance. It should be noted that the segment analysed in this first part of the study corresponds to the lower part of the arch dam, where the greater thickness minimizes slippage and joint openings. The second part of the study, titled "*Numerical experiment for shear key joint behaviour simulation in arch dams: Part 2 – Investigating the influence of the arch thickness and applied force*", will examine an upper dam segment, highlighting the need of incorporating arch thickness as a critical parameter in future analyses. It is particularly important to evaluate the role of arch thickness in influencing tangential stiffness for identical shear key configurations. Additionally, the second part of the study will also explore the effects of varying applied forces.

The research confirms the efficiency of the proposed approach in simulation of the complex nonlinear behavior of an arch dam constructed with shear key joints, eliminating the need for explicit geometric modeling. The model will be applied to simulate contraction joints in an arch dam, evaluating the impact of the different joint types on stress redistribution and the overall structural response under static and dynamic loading conditions.

References

[1] Talatahari, S., Salami M., Parsiavash, R. (2016): Optimum design of double curvature arc dams using a quick hybrid charged system search algorithm. *Iran University of Science & Technology*, **6**, 227-243, Corpus ID: 53392743.

[2] Du, C. B., Jiang, S. Y. (2010): Effects of contraction joints and key slots on the seismic responses of arch dam (in Chinese). *Journal of Hydroelectric Engineering*, **29** (5), 1–5.

[3] Ahmadi, M. T., Izadinia, M., Bachmann, H. (2001): A discrete crack joint model for nonlinear dynamic analysis of concrete arch dam. *Computers and Structures,* **79** (4), 403-420, https://doi.org/10.1016/S0045-7949(00)00148-6.

[4] Fenves, G. L., Mojtahedi, S., Reimer, R. B. (1992): Effect of contraction joints on earthquake response of an arch dam. *Journal of Structural Engineering*, **118** (4), 1039—1055, https://doi.org/10.1061/(ASCE)0733-9445(1992)118:4(1039).

[5] Lau, D. T., Noruziaan, B., Razaqpur, A. G. (1998): Modelling of contraction joint and shear sliding effects on earthquake response of arch dams. *Earthquake Engineering and Structural Dynamics*, **27**, 1013-1029, https://doi.org/10.1002/(SICI)1096-9845(199810)27:10<1013::AID-EQE765>3.0.CO;2-0.

[6] Tzenkov, A. D., Lau, D. T. (2002): Seismic analysis of concrete arch dams with contraction joints and non-linear material models, *7th U.S. National Conference on Earthquake Engineering*, Boston, Massachusetts.

[7] Toyoda, Y., Ueda M., Shiojiri, H. (2002): Study of joint opening effects on the dynamic response of an existing arch dam, *15th ASCE Engineering Mechanics Conference*, Columbia University, New York.

[8] Noble, C. R., Solberg J. (2004): Nonlinear seismic analysis of Morrow Point dam. *A Study for the United States Bureau of Reclamation*, UCRL-TR-202545.

DOI: https://doi.org/10.5592/CO/3CroCEE.2025.111

[9] Guerra, A. (2007): Shear key research project – Literature review and finite element analysis. Dam Safety Technology Development Program, U.S. Department of the Interior, Bureau of Reclamation, *Report DSO-07-05*.

[10] Ricketts, R. E. Zienkiewicz, O. C. (1975): *Preformed 'cracks' and their influence on behaviour of concrete dams*. Criteria and assumptions for numerical analysis of dams, UK.

[11] Row, D., Schricker, V. (1984): Seismic analysis of structures with localized nonlinearities, *8th World Conference on Earthquake Engineering*, San Francisco, California.

[12] O' Connor, J. P. F. (1985): The modeling of cracks, potential crack surfaces and construction joints in arch dams by curved surface interface elements, *15th International Conference on Large Dams*, Lausanne, Switzerland.

[13] Beer, G. (1985) An isoperimetric joint/interface element for finite element analysis. *International Journal for Numerical Methods in Engineering*, **21**, 585-600, https://doi.org/10.1002/nme.1620210402.

[14] Dowling, M. J., Hall, J. F. (1989): Nonlinear seismic analysis of arch dams. *Journal of Engineering Mechanics, ASCE*, **115** (4), 768-89, https://doi.org/10.1061/(ASCE)0733-9399(1989)115:4(768).

[15] Ahmadi, M. T., Razavi, S. (1992): A three-dimensional joint opening analysis of an arch dam. *Computers and Structures*, **44** (1-2), 187–192, https://doi.org/10.1016/0045-7949(92)90237-T.

[16] Lotfi, V. (1996): Comparison of discrete crack and elasto-plastic models in nonlinear dynamic analysis of arch dams. *Dam Engineering*, **7** (1).

[17] Mays, J. R., Roehm, L. H. (1993): Effect of vertical contraction joints in concrete arch dams. *Computers & Structures*, **47** (4-5), 615-627, https://doi.org/10.1016/0045-7949(93)90346-F.

[18] Azmi, M., Paultre P. (2002): Three-dimensional analysis of concrete dams including contraction joint non-linearity. *Engineering Structures*, **24**, 757–771, https://doi.org/10.1016/S0141-0296(02)00005-6.

[19] Arabshahi, H. R., Lotfi, V. (2009): Nonlinear dynamic analysis of arch dams with joint sliding mechanism. *Engineering Computation*, **26** (5), 464–482, https://doi.org/10.1108/02644400910 970158.

[20] Wang, J. T., Jin, F., Zhang, C. H. (2011): Seismic safety of arch dams with aging effects. *Science China Technological Sciences*, **54** (3), 522–530.

[21] Du, C. B., Jiang, S. Y. (2010): Effects of contraction joints and key slots on the seismic responses of arch dam (in Chinese). *Journal of Hydroelectric Engineering*, **29** (5), 1–5.

[22] Jiang S. Y., Du C. B., Yuan, J. W. (2011): Effects of shear keys on nonlinear seismic responses of an arch – gravity dam. *Technological Sciences*, Science China Press and Springer, Verlag Berlin 2011.

[23] ADAD-IZIIS – Software for analysis and design of arch dams. *Institute of Earthquake Engineering and Engineering Seismology*, University of Ss. Cyril and Methodious, Skopje, R. N. Macedonia.